Available online at www.sciencedirect.com
SCIENCE DIRECT
Materials Chemistry and Physics 92 (2005) 534–539
MATERIALS CHEMISTRY AND PHYSICS
www.elsevier.com/locate/matchemphys

Synthesis, characterization and thermal stability of Ni_3P coatings on nickel

Heriberto Pfeiffer [a,*], Franck Tancret [b], Thierry Brousse [b]

[a] *Instituto de Investigaciones en Materiales, Universidad Nacional Autónoma de México, Circuito Exterior s/n C. U., Apartado postal 70-360, Coyoacan 04510, México, D.F., Mexico*
[b] *Laboratoire de Génie des Matériaux, Ecole Polytechnique de l'Université de Nantes, BP50609, 44306 Nantes Cedex 3, France*

Received 22 October 2004; received in revised form 13 January 2005; accepted 30 January 2005

Abstract

The reaction mechanism describing the formation and surface decomposition of Ni_3P has been investigated. Ni_3P was synthesized as a thick film on a Ni foil by a simple solid-state reaction. X-ray diffraction confirms that the layer produced, on the surface of the Ni foil, is pure Ni_3P. The solid-state reaction did not occur at 400 °C or lower temperatures. At 600 °C or higher temperatures the solid-state reaction occurred by a nucleation mechanism of synthesis and later sintering of Ni_3P particles at the surface of the Ni foil. The surface of the Ni_3P–Ni foil showed to be stable in air up to 300 °C. At higher temperatures, Ni_3P decomposed trough a complex mechanism, including the loss of phosphorus, the formation of the phases $Ni_{12}P_5$ and Ni_2P, and finally, oxidation of the nickel phosphides. Samples heated at 800 °C for 4 h produced a NiO layer on the surface of the Ni_3P–Ni foil.
© 2005 Elsevier B.V. All rights reserved.

Keywords: Ceramics; Ni_3P coating on Ni; Oxidation; Thermal properties; Ni_3P; Ni_2P; $Ni_{12}P_5$

1. Introduction

Nickel phosphides are of research interest because of their technological applications. For example, these materials are well known as corrosion-resistant, wear-resistant and waterproof materials [1–3]. Furthermore, in recent years, there has been research on their application as composite layer materials as magnetic wear-resistant coatings on hard-disk substrates and for catalytic purposes as well [4–7].

Although there are several nickel phosphides reported in the literature, the stoichiometry of many of these compounds is uncertain. In most cases, the accuracy with which their composition is defined, improves as the phosphorus content decreases [8,9]. Ni_3P, which is the nickel phosphide with the smallest content of phosphorus, has a tetragonal crystal structure with $a = 8.954$ Å and $c = 4.386$ Å [10]. Ni_3P is usually synthesized successfully by electrochemical deposition [11,12]. Nevertheless, this material has been also produced by complex chemical reactions [5,13].

Electroless nickel plating has been proposed as a hard coating for industrial applications [11]. Using this technique, the coating obtained is a mixture of Ni and Ni_3P, where the maximum content of Ni_3P depends on the pH value of the electroless solution. However, the relatively poor thermal stability of Ni–P deposits is a critical issue. The formation of Ni and Ni_3P crystals may cause the degradation of mechanical properties in the coating. Actually, there is relatively little work reported on the mechanism of synthesis and thermal stability of this compound.

Recently, different metal phosphides have been synthesized by a new and very simple process, involving a solid-state reaction [14]. Then, the aim of this study was to analyze in detail the synthesis of Ni_3P by this new method and thermal stability of Ni_3P as well. To achieve this, X-ray diffraction and scanning electron microscopy have been used to monitor the reaction progress as a function of heat treatment temperature.

* Corresponding author. Tel.: +52 55 5622 4641; fax: +52 55 5616 1371.
E-mail address: pfeiffer@zinalco.iimatercu.unam.mx (H. Pfeiffer).

0254-0584/$ – see front matter © 2005 Elsevier B.V. All rights reserved.
doi:10.1016/j.matchemphys.2005.01.055

2. Experimental details

For the synthesis of Ni_3P, red phosphorous (Aldrich) was suspended in ethanol. Then, the phosphorus suspension was sprayed on a Ni foil previously heated at 70 °C. Once the ethanol was evaporated, a red-black film was produced on the Ni foil. This procedure was already used to produce different metallic phosphides [14]. A set of these "Ni–P" foils was heat-treated at 400 °C for 8 h, under flowing Ar:H_2 (95:5 ratio). Another set of samples was sealed in silica tubes under vacuum. The sealed tubes were heat-treated in an electrical furnace. After heat treatment, the samples were removed from the furnace and air-quenched. On the other hand, for the thermal stability analysis, the Ni_3P–Ni foils were heat-treated between 300 and 800 °C in air. In this case, after the thermal treatment, the samples were removed from the furnace and air-cooled down.

The samples were characterized by X-ray diffraction (XRD) and scanning electron microscopy (SEM). The XRD patterns were recorded with a Siemens D5000 diffractometer, using a Cu $K\alpha_1$ anode. The percentages of the various compounds present in the foils were estimated from the total area under the most intense diffraction peak for each phase identified, with the assumption these values were proportional to the volume fraction of each compound. In this way, the amounts of the crystalline compounds present in the samples were obtained within an estimated experimental error of ±3%. SEM (Leo, Stereoscan 440) was used to characterize the particle size and morphology of the materials. The microscope was coupled with an energy-dispersive X-ray analyzer (Link Isis, Oxford Instrument). Finally, a thermogravimetric analysis (TGA) was performed with a heating rate of 5 K min^{-1} (TG 209 Thermische Analyse, Netzsch). This analysis was performed in order to investigate the thermal stability of Ni_3P in air.

3. Results and discussion

3.1. Synthesis and characterization of Ni_3P

In order to determine the process of Ni_3P synthesis, samples were heat-treated for 8 h between 400 and 800 °C. First, a "Ni–P" foil was heat-treated at 400 °C for 8 h, in flowing Ar:H_2. The XRD pattern, from the surface of this sample, did not show the formation of Ni_3P. This sample only showed metallic Ni (JCPDS file No. 87-0712) [15].

Indeed, the red phosphorus sublimates at 416 °C [16], so that heat treatments at higher temperatures had to be performed in sealed tubes to avoid the loss of phosphorus. Samples were heat-treated at 600 and 800 °C for 8 h. Both samples produced a grey-metallic film on the surface of the Ni foil. These grey-metallic films were stable in air. A typical XRD pattern from the "Ni–P" foil heat-treated at 800 °C for 8 h is shown in Fig. 1. Ni_3P was the main phase and only metallic Ni was detected as secondary phase. It must correspond to

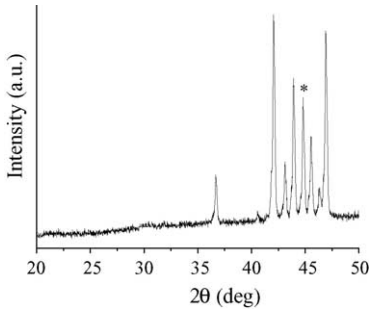

Fig. 1. XRD pattern of a sample heat-treated for 8 h at 800 °C. Asterisk (*) indicates that the peak corresponds to the Ni foil.

the Ni foil substrate, on which Ni_3P is supported. Hence, the phosphorus, in gas form, reacts with the Ni foil according to reaction (1). In this case, as nickel is in excess, the nickel phosphide expected is that with the highest Ni/P ratio

$$3Ni + P_{(g)} \rightarrow Ni_3P \quad (1)$$

A SEM image of the Ni_3P produced at 800 °C is shown in Fig. 2. Close examination shows that the film was produced from a crystal growth of the Ni_3P particles and its consequent sintering. The degree of sintering seems to be very high due to the high contact area between the particles. Furthermore, it is obvious that all the pores were produced by the conjugation of several necks formed during the sintering process.

In order to better understand the synthesis and sintering mechanisms of Ni_3P, other samples were heat-treated at 600 °C for 0.5, 2 and 6 h. Only Ni_3P and Ni were detected by XRD analysis, even after 30 min of thermal treatment. However, SEM analysis showed inhomogeneities and impurities in the film, when it was heat-treated for short times. Fig. 3 shows SEM images of Ni_3P films heat-treated for different times at 600 °C. After 30 min of heat-treatment (Fig. 3a), the surface of the Ni foil presented areas of different compositions. While some nucleation centres of Ni_3P could be detected, there were areas where just the Ni foil was found. Furthermore, phosphorus seemed not to be anymore homogeneously deposited on the surface of the Ni foil. It can be

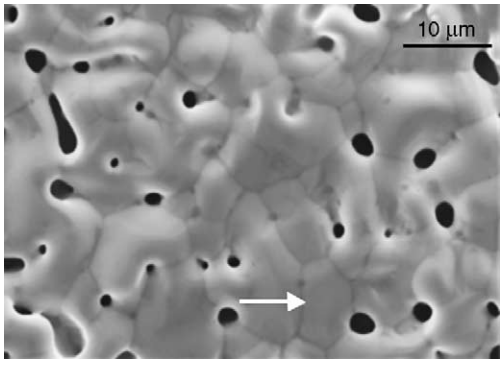

Fig. 2. SEM image of Ni_3P produced at 800 °C. The arrow indicates the contact area between two different particles produced during the sintering process.

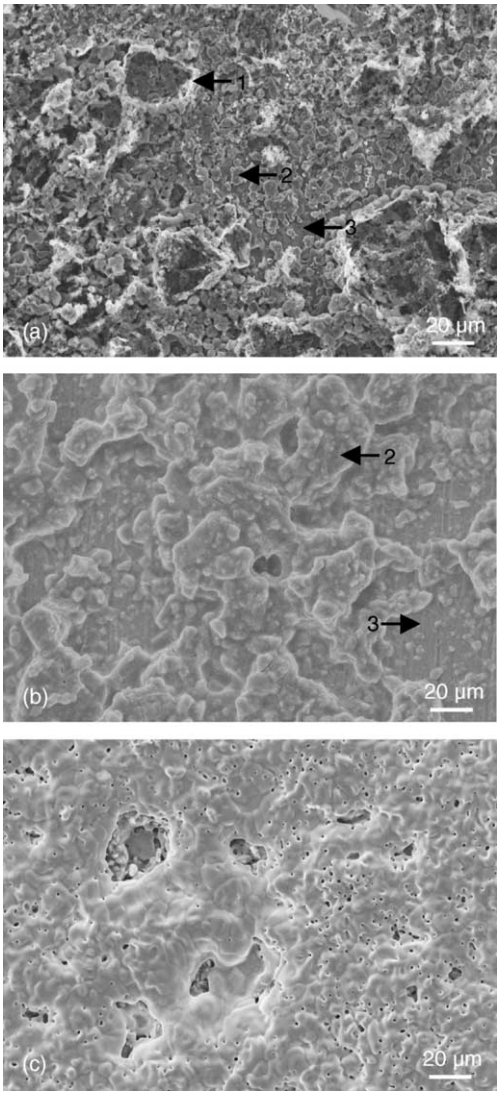

Fig. 3. SEM images of samples heat-treated at 600 °C for 30 min (a), 2 h (b) and 6 h (c). EDS analysis of zone 1 showed a high content of P (50 at.%). The analysis of zone 2 is in an excellent agreement with the Ni_3P composition (27 at.% P and 73 at.% Ni). On the other hand, zone 3 is mainly Ni.

due to the phosphorus sublimation and later deposition during the quench process of the sealed tube. EDS analysis of the different zones of this sample gave the following results (zones are labelled in Fig. 3a). Zone 1 gave high values of phosphorus, around 50 at.% (brighter particles). On the other hand, zone 2 gave on average the following result; 27 at.% P and 73 at.% Ni. These values are in a good agreement with the Ni_3P composition. Finally, zone 3 gave very poor values of phosphorus, in some cases, it could not be detected. Although EDS results have to be analyzed carefully, apparently after 30 min, some Ni_3P particles were already produced, but the reaction between nickel and phosphorus had not been completed.

SEM images of samples heat-treated for 2 and 6 h are shown in Fig. 3b and c, respectively. Phosphorus was not detected in high concentrations in the sample heat-treated for

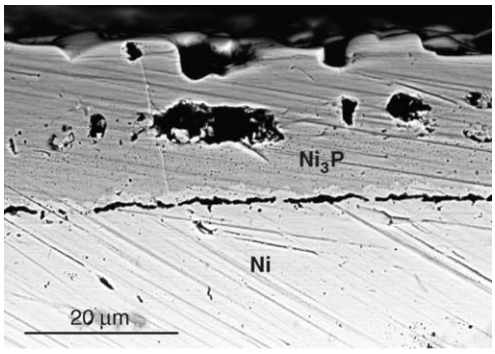

Fig. 4. BSEI image of the cross-section of a Ni_3P–Ni foil heat-treated at 800 °C for 8 h. EDS analysis: Surface phase 78 at.% Ni and 22 at.% P; bulk phase 96 at.% Ni and 3 at.% P.

2 h, in comparison with those samples heat-treated for just 30 min. Furthermore, EDS analysis only showed two different compositions: pure Ni (from the Ni foil) and Ni_3P. Apparently, the reaction between nickel and phosphorus was already finished after this time. The only difference between the samples heat-treated for 2 and 6 h was in the morphology of the films. The surface of the sample heat-treated for 2 h presented an inhomogeneous morphology. Ni_3P was not homogeneously and totally distributed, there were some areas where the Ni foil was not covered by Ni_3P (Fig. 3b). On the other hand, the sample heat-treated for 6 h presented a homogeneous morphology and the Ni foil was totally covered (Fig. 3c). This result is close to the morphology observed in the films heat-treated at 800 °C.

Fig. 4 shows the backscattered electron image (BSEI) of the cross-section of a Ni_3P–Ni foil. This figure confirms the presence of two different phases in the surface region. The difference in contrast seen in this image arises from the differences in mean atomic number, $\bar{Z}$, of Ni ($\bar{Z} = 28$) and Ni_3P ($\bar{Z} = 24.75$), giving rise to a difference in the backscattered electron coefficient, η, of the two phases through the equation [17]:

$$\eta = -0.0254 + 0.016\bar{Z} - 1.86 \times 10^{-4}\bar{Z}^2 + 8.3 \times 10^{-7}\bar{Z}^3 \quad (2)$$

η decreases from 0.294 for Ni, the brighter phase in Fig. 4, to 0.269 for Ni_3P, the darker phase. Furthermore, EDS analyses were in excellent agreement with the BSEI images. The Ni/P ratio was 3 for the darkest phase. This composition corresponds to the Ni_3P stoichiometry. On the other hand, the brighter phase almost did not contain any phosphorus (3 at.%) meaning that this phase is just metallic Ni.

The thickness of the Ni_3P external layer was around 20 ± 5 μm, and the film contained pores with different sizes. These pores must be produced during the sintering process, as already described above. Furthermore, the presence of a fracture along the Ni_3P/Ni interface is evident. This fracture must be produced by a mechanical stress at the interface of the Ni_3P–Ni foil. Furthermore, the thermal expansion coefficients of metals are usually larger than those of ceramics [16].

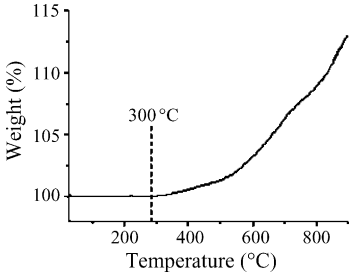

Fig. 5. Thermogravimetric analysis of Ni_3P powder mechanically scratched from the Ni_3P–Ni foil.

In this case, the thermal expansion coefficient of Ni_3P, a ceramic, has not been reported. However, it can be assumed that its thermal expansion coefficient is much smaller than that for Ni ($13 \times 10^{-6}\,K^{-1}$). Then, the difference in expansion when the samples were cooled down could produce high stresses at the interface, causing a fracture in this part of the material. Creating this kind of fracture is analogous to the creation of a gap during high-temperature oxidation of a metal [18]. Furthermore, this phenomenon has already been seen during the synthesis of other metallic phosphides. Nowacki [19] reported a similar result during the synthesis of iron phosphides.

3.2. Thermal stability of the Ni_3P–Ni foil

A thermogravimetric analysis (TGA) of Ni_3P was performed, in order to know the thermal stability of the material in air. A TGA curve from room temperature to 900 °C, for the Ni_3P mechanically scratched from the surface of the Ni foil, is shown in Fig. 5. The weight of the sample began to change beyond 300 °C, and the overall increase of weight was 13% of the initial weight. Apparently, an oxidation process begins at 300 °C. In order to do a better analysis of the thermal stability of Ni_3P, in an oxidative environment, a set of Ni_3P–Ni samples were heat treated between 300 and 800 °C at 100 K intervals for 4 h. XRD results from the surfaces of the Ni_3P–Ni foils after various heat treatments are shown in Fig. 6.

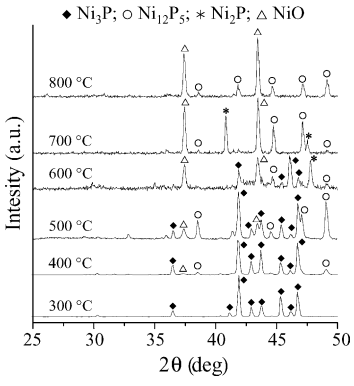

Fig. 6. XRD patterns of the Ni_3P–Ni foils heat-treated for 4 h at various temperatures.

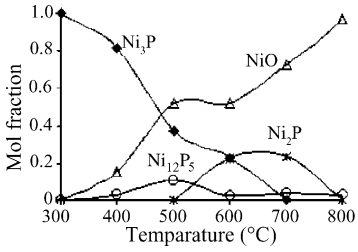

Fig. 7. Mol fractions of Ni_3P, $Ni_{12}P_5$ Ni_2P and NiO as a function of temperature.

The sample heat-treated at 300 °C only showed the presence of Ni_3P (JCPDS file No. 74-1384) [10]. It is in good agreement with the TGA showing that the Ni_3P–Ni foil is stable up to 300 °C. By contrast, small amounts of NiO (15 mol%) and $Ni_{12}P_5$ (3 mol%) (JCPDS file Nos. 78-0643 and 74-1381, respectively) [10,20] could be detected on the surface of the sample heat-treated for 4 h at 400 °C (Fig. 7). The remainder of the foil surface was Ni_3P, 82 mol%. The formation of the metastable phase $Ni_{12}P_5$ is consistent with a partial oxidation of the Ni_3P according the following reaction:

$$5Ni_3P + \tfrac{3}{2}O_2 \rightarrow 3NiO + Ni_{12}P_5 \quad (3)$$

Increasing the heat treatment temperature to 500 °C caused an important change in the composition of the material, which changed to 11 mol% $Ni_{12}P_5$, 37 mol% Ni_3P and 52 mol% NiO. Conversely, Ni_2P appeared in the sample heat-treated at 600 °C, 23 mol% at this temperature. The rest of the composition was 23 mol% of Ni_3P, 3 mol% of $Ni_{12}P_5$ and 51 mol% of NiO. Ni_2P could be produced from a partial oxidation of Ni_3P and/or $Ni_{12}P_5$ (reactions (4) and (5))

$$Ni_3P + \tfrac{1}{2}O_2 \rightarrow Ni_2P + NiO \quad (4)$$

$$Ni_{12}P_5 + O_2 \rightarrow 5Ni_2P + 2NiO \quad (5)$$

Something interesting in this case is that the formation of Ni_2P is associated with the decrease of $Ni_{12}P_5$ and a partial stabilization of Ni_3P (Fig. 7). It strongly suggests that Ni_2P is produced by the partial oxidation of both phosphides Ni_3P and $Ni_{12}P_5$.

Samples heat-treated at 700 and 800 °C changed the relative proportions of the phases, Ni_3P, $Ni_{12}P_5$ Ni_2P and NiO, found on the surface of the samples, as shown in Fig. 7. At 700 °C, the proportion of Ni_3P declined to zero and the NiO increases up to 72 mol%. In this case, the quantities of Ni_2P (24 mol%) and $Ni_{12}P_5$ (4 mol%) were similar to those values found at 600 °C. Finally, NiO was the main product found at 800 °C, 97 mol%, and only 3 mol% of $Ni_{12}P_5$ was detected.

According to reaction (3), the quantities of NiO should be three times higher than those of $Ni_{12}P_5$. However, at 400 and 500 °C, the NiO quantities are five times the $Ni_{12}P_5$ quantities. This difference can be explained by a partial oxidation of $Ni_{12}P_5$ (reactions (6) and (7)), which obviously increases the NiO amounts. According to reaction (6), some phosphorus is produced during the $Ni_{12}P_5$ oxidation. On the other hand,

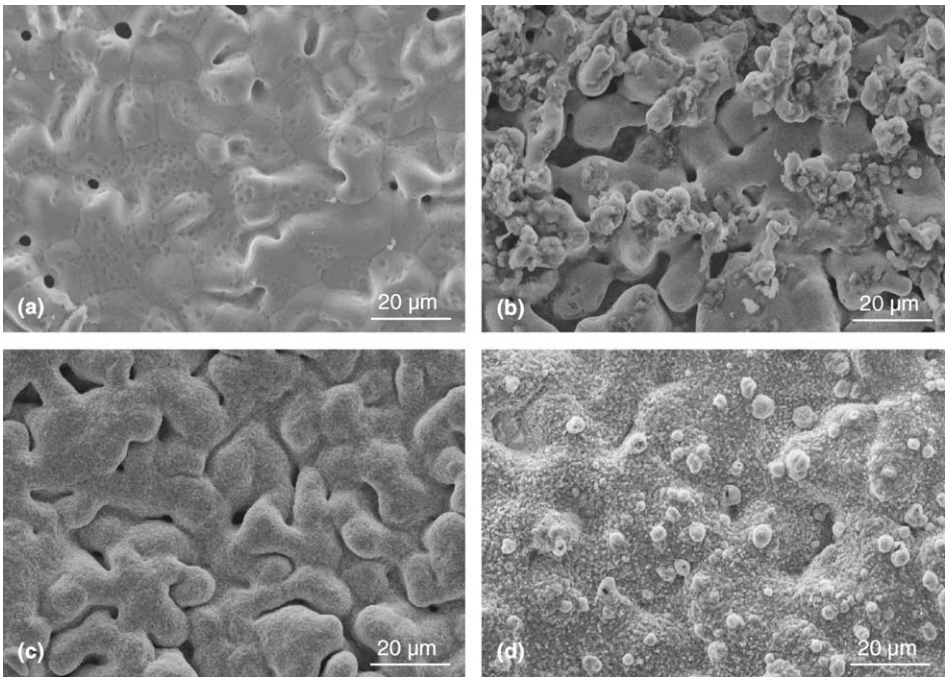

Fig. 8. SEM images of the Ni_3P–Ni foils heat-treated for 4 h at various temperatures: (a) 500 °C, (b) 600 °C, (c) 700 °C and (d) 800 °C.

reaction (7) shows an oxidation of nickel and phosphorus to produce NiO and phosphorus oxide (P_2O_5). P_2O_5 sublimates at 360 °C. Then, phosphorus may sublimate directly or through a reaction with oxygen

$$Ni_{12}P_5 + 6O_2 \rightarrow 12NiO + 5P \quad (6)$$

$$2Ni_{12}P_5 + \tfrac{49}{2}O_2 \rightarrow 24NiO + 5P_2O_5 \quad (7)$$

At 700 °C, while Ni_3P totally disappeared, NiO increased its molar fraction up to 72 mol%. As for the previous temperatures, NiO is produced by the oxidation of the three different nickel phosphides, Ni_3P, $Ni_{12}P_5$ and/or Ni_2P. In these cases, the oxidation could be produced by any of the different reactions mentioned above or by the following reactions ((8)–(11)):

$$Ni_3P + \tfrac{3}{2}O_2 \rightarrow 3NiO + P \quad (8)$$

$$Ni_2P + O_2 \rightarrow 2NiO + P \quad (9)$$

$$2Ni_3P + \tfrac{11}{2}O_2 \rightarrow 6NiO + P_2O_5 \quad (10)$$

$$2Ni_2P + \tfrac{9}{2}O_2 \rightarrow 4NiO + P_2O_5 \quad (11)$$

Finally, at 800 °C, nickel phosphides were almost not detected. Hence, a complete oxidation is reached at this temperature.

SEM images of the Ni_3P–Ni foils heat-treated between 500 and 800 °C for 4 h are shown in Fig. 8. The sample heat-treated at 500 °C (Fig. 8a) did not show any significant changes in comparison with the pristine material (see Fig. 2). Although the shape of the surface did not change, there was the formation of tiny concave "spots" all over the surface. XRD analysis of this sample showed the presence of NiO and $Ni_{12}P_5$. Then, these "spots" may be the nucleation centres of NiO and/or $Ni_{12}P_5$. When the samples were heated up to 600 °C (Fig. 8b), the morphology of the surface presented a significant change. In this case, it was possible to see the formation of agglomerates all over the surface. The size of these agglomerates ranged between 5 and 50 μm. Furthermore, the EDS analysis of these agglomerates suggests that they are mainly NiO (Ni = 48 at.%, O = 49 at.% and P = 3 at.%). At 700 °C, the agglomerates disappeared and the whole surface became noticeably rougher in appearance (Fig. 8c). This rough surface is NiO, according the EDS analysis that gave very similar results to those showed for the agglomerates. Finally, the surface of the sample heat-treated at 800 °C (Fig. 8d) looks like an extreme case of the previous sample (Fig. 8c). The surface was totally covered by NiO, with the formation of many spherical NiO particles of 2−5 μm in size. These particles seem to be the product of a continuous growth of NiO on the surface. Furthermore, the surface did not show the pores that were present before.

On the other hand, Fig. 9 shows the cross-section of the sample heat-treated at 800 °C for 4 h. The XRD results showed NiO as the main phase (97%). However, this figure shows that not all the nickel phosphide phase was converted to NiO. A NiO film, 2–3 μm thick, can be seen on the top of Ni_3P–Ni phase, and the rest of the film must be a mixture of nickel phosphides and NiO, according to the EDS analyses. Furthermore, the pores in the nickel phosphide phase presented the same oxidation as on the external surface. Then, most of the pores must be connected to the surface, allowing their oxidation.

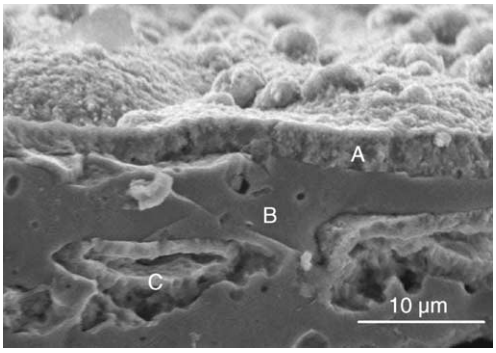

Fig. 9. SEM image of the cross-section of a Ni_3P–Ni foil heat-treated at 800 °C for 4 h in air. EDS results were as follows: (A) 50 at.% Ni, 47 at.% O and 3 at.% P; (B) 60 at.% Ni, 22 at.% O and 18 at.% P; (C) 47 at.% Ni, 48 at.% O and 5 at.% P.

X-ray diffraction from scratched and pulverised powder taken from the Ni_3P–Ni foil heat-treated at 800 °C showed the following composition: 35 mol% $Ni_{12}P_5$, 31 mol% NiO, 18 mol% Ni_2P and 15 mol% Ni_3P. This result is in excellent agreement with the analyses done by EDS. Thus, the difference between the X-ray analysis from the layer and the powder, of the same sample, can be attributed to the NiO surface layer produced during the thermal treatment. As the last sample is composed of a thick surface layer (2–3 μm), underneath which there is a bulk material (nickel phosphides), the relative intensities of X-ray from the bulk material must be reduced and the intensities of the X-ray from the surface is enhanced because of the NiO absorption [21]. This can explain why the X-ray analysis of the surface of the foil heat treated at 800 °C for 4 h almost only showed NiO.

According to these results, Ni_3P decomposes at high temperatures in air, through a complex mechanism. First, there is a partial oxidation related with the formation of different nickel phosphides ($Ni_{12}P_5$ and Ni_2P). After that, an oxide film of NiO is produced all over the surface of the samples. Then, these results may help to establish the limit thermal conditions in which Ni_3P may be used and the possible consequences (the oxidation degree), if the material is used at higher temperatures.

4. Conclusions

Ni_3P was synthesized as a thick film on a Ni foil by a solid-state reaction, using a simple method. Temperature and time were found to be important factors in the reaction mechanism of Ni_3P synthesis and its subsequent decomposition. The solid-state reaction between the Ni foil and phosphorus did not occur at 400 °C or lower temperatures. The synthesis of the material was done at 600 °C or higher temperatures. A study of the evolution of the Ni_3P formation on the Ni foil showed that Ni_3P is produced by a nucleation mechanism; later on sintering and homogenisation of Ni_3P occur at the surface of the Ni foil.

The Ni_3P–Ni foil decomposed when it was heat-treated at 400 °C or higher temperatures in air. Ni_3P decomposes trough a complex mechanism, including the loss of phosphorus. Phosphorus must sublimate as element or as P_2O_5. Furthermore, during the thermal treatment there was the formation of different phosphides like the metastable $Ni_{12}P_5$ and Ni_2P phases. Finally, the oxidation of the different nickel phosphides takes place. Ni_3P–Ni foils heat-treated for 4 h at 800 °C produced a thick shell of NiO on their surfaces.

This work helps to better understand the mechanism of the Ni_3P synthesis and its thermal decomposition in air. Furthermore, this kind of studies may allow optimising and developing new industrial applications for Ni_3P.

Acknowledgement

H. Pfeiffer thanks to the Région des Pays de la Loire France, for financial support, during his postdoctoral position at the University of Nantes.

References

[1] H.L. Su, Y. Xie, B. Li, X.M. Liu, Y.T. Qian, Solid State Ionics 122 (1999) 157.
[2] H.S. Yu, S.F. Luo, Y.R. Wang, Surf. Coat. Technol. 148 (2001) 143.
[3] W.Y. Chen, J.G. Duh, Surf. Coat. Technol. 177/178 (2004) 222.
[4] D.Y. Ding, J.N. Wang, Z.L. Cao, J.H. Dai, F. Yu, Chem. Phys. Lett. 371 (2003) 333.
[5] S.J. Sawhill, D.C. Phillips, M.E. Bussell, J. Catal. 215 (2003) 208.
[6] S.T. Oyama, J. Catal. 216 (2003) 343.
[7] B. Bozzini, V.E. Sidorov, A.S. Dovgopol, J.P. Birukov, Int. J. Inorg. Mater. 2 (2000) 437.
[8] M.E. Schlesinger, Chem. Rev. 102 (2002) 4267.
[9] C.E. Myers, T.J. Conti, J. Electrochem. Soc. 132 (1985) 454.
[10] E. Larsson, Ark. Kemi. 23 (1965) 335.
[11] K.G. Keong, W. Sha, S. Malinov, J. Alloys Comp. 334 (2002) 192.
[12] M. Saitou, Y. Okudaira, W. Oshikawa, J. Electrochem. Soc. 150 (2003) 140.
[13] C.Y. Wang, Y. Zhou, Y.R. Zhu, Y. Hu, Z.Y. Chen, Mater. Sci. Eng. B 77 (2000) 135.
[14] H. Pfeiffer, F. Tancret, M.P. Bichat, L. Monconduit, F. Favier, T. Brousse, Electrochem. Commun. 6 (2004) 263.
[15] H.E. Swanson, E. Tatge, Natl. Bur. Stand. 539 (1953) 359.
[16] R.C. Weast, M.J. Astle, Handbook of Chemistry and Physics, 61st ed., CRC Press, New York, 1981.
[17] J.I. Goldstein, D.E. Newbury, P. Echlin, D.C. Joy, E. Fiori, Scanning Electron Microscopy and X-ray Microanalysis, Plenum Press, New York, 1981, 75–77.
[18] J. Nowacki, Wear 173 (1994) 51.
[19] J. Nowacki, Surf. Coat. Technol. 151/152 (2002) 114.
[20] N.G. Schlmahl, J. Barthel, G.F. Eikerling, Z. Anorg, Allg. Chem. 332 (1964) 230.
[21] A.C.J. Wilson (Ed.), International Tables for Crystallography, vol. C, 4th ed., Kluwer Academic Publishers, Dordrecht, 1995, pp. 200–202.